

# Dynamics of mode formation in an open resonator

Vladimir G. Niziev\* and Roman V. Grishaev

Institute on Laser and Information Technologies, Russian Academy of Sciences,  
Shatura, Moscow Region 140700, Russia

\*Corresponding author: niziev@yahoo.com

Received 1 July 2010; revised 12 October 2010; accepted 15 October 2010;  
posted 21 October 2010 (Doc. ID 130768); published 22 November 2010

We developed an iteration algorithm for open resonator simulation and employed it in studying the dynamics of mode formation. Simulations of an axially symmetrical empty resonator rely on an analytical description of radiation diffraction from a narrow ring. Reflection of an incident wave with a specified amplitude-phase distribution from the mirror is calculated by the Green function method. The process of mode formation is characterized by relaxation oscillations of various frequencies depending on the resonator parameters. The evolution of the relaxation oscillation amplitude can be aperiodic in nature, or it can occur as beats of a different frequency. It has been shown that there is a consistency between the known conditions of paraxial resonance obtained in the approximation of geometric optics and the aperiodic processes of evolution of relaxation oscillation amplitude in mode forming. An investigation has been performed on the factors affecting the time of mode formation. The possibility has been shown for multipass mode suppression and  $TEM_{10}$  mode generation by the use of an absorber mask on the resonator mirror. © 2010 Optical Society of America  
*OCIS codes:* 140.3410, 030.4070.

## 1. Introduction

The problem of optical resonator simulation has been considered repeatedly, both analytically and numerically. It was the subject of fundamental work done nearly 50 years ago [1,2]. Many known monographs offer evidence of the systematic treatment of this problem [3–6]. A classical statement of the problem consists in the description of the resonator modes. Of special interest in the wide scope of practical applications are transverse modes, which determine radiation structure in the beam cross section. The analytical descriptions of Laguerre–Gaussian (LG) modes for round mirrors are well known (e.g., [7]). They have been obtained as self-reproduced solutions to the scalar wave equation in the paraxial approximation. The classical works on resonator numerical simulation also reveal that any initial distribution of a field is transformed to a Gaussian beam after multiple reflections from the resonator mirrors. Up-to-date numerical calculations generally propose

to describe the structure of laser radiation with regard to the features of both the resonator and the active medium. Despite the great number of works in the field of open resonators, this problem cannot be regarded as a solved one. Even in low-power cw lasers possessing high-quality resonators, generation of an individual nonprincipal LG mode is rather problematic. It can be obtained experimentally only by using special measures; see, for example, the recent article [8]. The authors obtained the generation of high-order modes in a laser with pulse energy of  $\sim 10$  mJ, and they used a phase mask and passive  $Q$  switch for this purpose. On the market one can only find either main mode lasers or “multimode” lasers having an uncertain field structure in the beam cross section. In most cases the conditions of laser generation are far from ideal, so the conclusions of classical theory are made with a high degree of approximation.

There exists a broad class of high-power lasers featuring high gain in the active medium and a low-quality resonator. The output beam quality in these lasers is expected to depend on the time of the transverse mode formation in the resonator. If this time is

---

0003-6935/10/346582-09\$15.00/0  
© 2010 Optical Society of America

long, there can be no hope for a quality close to the ideal beam.

Another example is from the area of pulsed (or pulse-periodic) lasers. As the transverse structure of the radiation starts to be formed in each of the pulses, it is required that the time of mode formation in the selected resonator is compared with the laser pulse duration for the beam quality to be generally characterized. In present-day pulsed lasers, the pulse duration can range from femtoseconds to milliseconds. Both examples are indicative of the cognitive and practical expediency of studying the process of transverse mode formation in laser resonators.

Along with the generally accepted wave approach to the description of transverse modes in a stable resonator, interesting works are available that are concerned with the peculiarities of the propagation of rays inside the stable resonator and done in the approximation of geometric optics. This places emphasis upon the relation between the wave and the geometric optics in describing stable resonators, upon single-pass (SP) wave LG modes and upon multipass (MP) geometric paraxial resonances. The authors of a fundamental paper on geometric optics of stable resonators [9] only mention this relation in the most general of expressions. This point also has not been touched upon in the above-cited monographs, which show a clear preference for the wave approach.

Mention should be made of a number of experimental and theoretical works devoted to “MP modes” [10–14]. The experiments produced specific conditions for excitation in these modes. A disk of  $\text{Nd}^{3+} : \text{YVO}_4$  1 mm thick and several millimeters in diameter was used as an active medium. The beam of a pump laser was displaced relative to the disk axis, and the pump area made less than 1% of the disk area. The Fresnel number for the resonators under study amounted to several tens and even hundreds. The authors attribute the MP modes to the superposition of higher order ordinary modes.

This work is aimed at the investigation of the factors affecting the time of attaining the field stationary distribution, the physical phenomena accompanying this process for various configurations of empty resonators, as well as the elucidation of the relationship between the conclusions resulting from the geometric and wave approaches to the analysis of stable resonators.

## 2. Mathematical Model

In all the problems to be solved below, we shall restrict ourselves to a description of axially symmetric solutions. This approximation is of current importance for many practical cases, as it is just under the axial symmetry of the resonator and active medium that the beam quality proves to be maximally high.

Our simulation algorithm is based on the Fox and Li iteration approach [1] and applied only for axially symmetric solutions. In this case the analytical solution of the diffraction problem for a narrow ring slit

can be used in the Green function method. A formal justification of applying the Green function approach to the case under consideration is given in Appendix A.

The diffraction field from an infinitely narrow ring of  $r_0$  radius is, for linear polarization at the distance  $L \gg r_0$ , expressed by the formula (see Appendix A)

$$\text{DEL}(L, \theta, r_0) \approx 2\pi r_0 i k \frac{e^{ikL}}{L} e^{ik\frac{r_0^2}{2L}} J_0(kr_0\theta). \quad (1)$$

Here,  $k$  is the wave vector and  $J_0$  is the zero-order cylinder Bessel function. The formula is valid at  $L \gg r_0$ . It is seen from the formula that, in the given approximations, the wavefront of the diffraction field is spherical. The phase is not dependent on the polar angle  $\theta$ ; though there is an extra phase shift depending on the emitting ring radius  $r_0$ .

The shapes of the surface where the initial field is specified and of that where the diffraction field is calculated can be different for convenience in calculating; see Fig. 1.

This may be a plane perpendicular to the resonator axis at the mirror location, the surface of the mirror itself, or the sphere of calculation. The radius of the sphere of calculation equals the resonator length. The amplitude-phase distribution of the field specified or obtained on any of these surfaces is readily recalculated to the amplitude-phase distribution on the other surface by phase correction, the amplitude being retained.

For an arbitrary amplitude-phase distribution of the initial field  $E_0(r_0)$ , the diffraction field at distance  $L$  is calculated by performing the integration

$$\begin{aligned} E(L, \theta) &\approx \int_0^{r_m} E_0(r_0) \text{DEL}(L, \theta, r_0) \exp\left(-ik\frac{r_0^2}{R}\right) dr_0 \\ &= 2\pi \frac{e^{ikL}}{L} \int_0^{r_m} r_0 E_0(r_0) \exp\left[\frac{ik}{2}\left(\frac{r_0^2}{L} - 2\frac{r_0^2}{R}\right)\right] \\ &\quad \times J_0(kr_0\theta) dr_0. \end{aligned} \quad (2)$$

This formula is written for the first iteration step, if the initial field  $E_0(r_0)$  is specified on the plane (see Fig. 1), and the diffraction field is calculated on the spherical surface of the  $L$  radius. These circumstances have an influence on the form of the

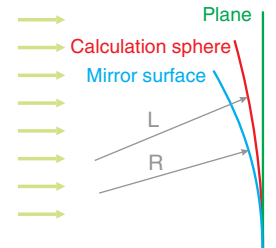


Fig. 1. (Color online) Explanation of the calculation procedure. The field can be specified (or calculated) on one of the three surfaces shown.

exponent multiplier in the integral. The phase emerges from the rings of different radii ( $r_0$ ) at the distance  $L$  [see (1)]; it is also related to the mirror curvature  $R$ . For the concave mirror, the sign of  $R$  is positive, and for the convex mirror it is negative. The other designations are  $r_m$ , mirror radius and  $L$ , distance between the mirrors.

All the consequent iteration steps except for the first one use the incident field specified on the spherical surface of the  $L$  radius, calculated at the previous step and give results on the same spherical surface. Then the exponent multiplier in the integrant has the following form:

$$\exp\left(ik \frac{r_0^2}{L} \left(1 - \frac{L}{R_i}\right)\right),$$

where  $i = 1, 2$  is the index specifying the resonator mirror.

The paraxial approximation defines a large class of practically important open resonators. In these resonators, the Fresnel number  $F = \frac{r_m^2}{\lambda L}$  is evaluated in unities. In expression (1) the phase term  $\sim \frac{r_0^2}{\lambda L}$  and the argument of the Bessel function are of the same order. They vary from zero to the Fresnel number  $F$  in the range of integrating over  $r_0$  from zero to the mirror radius  $r_m$ .

Expression (2) yields a formula for the field on the axis after reflection of a plane wave from a mirror of finite dimensions. In this particular case  $E_0(r_0) = \text{Const.}$ ,  $\theta = 0$ ,  $J_0(kr_0\theta) = 1$ , and the integral (2) is taken easily. The solution is conveniently written in the form

$$|E| \sim F \cdot \frac{\sin y}{y}; \quad y = \frac{\pi}{2} F \cdot (1 - 2L/R); \quad F = \frac{r_m^2}{\lambda L}. \quad (3)$$

Figure 2 illustrates the dependence of the amplitude of the field reflected from the mirror at its axis on the distance from the mirror. The field is at its maximum at the focus of the mirror  $L = R/2$ .

Another useful analytical formula can be derived for the case of  $R = 2L$ . Here the exponent in integral (2) is equal to 1. Formula (4) is obtained with the field produced on the sphere of  $L$  radius passing through the focus of the mirror:

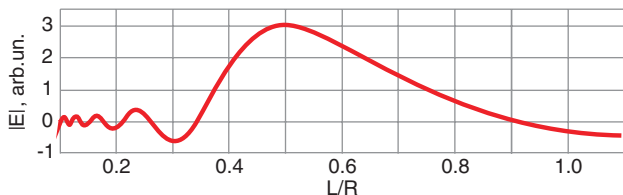


Fig. 2. (Color online) Amplitude of the field reflected from the mirror at its axis as a function of the distance from the mirror. Dimensionless parameters:  $r_m \cdot k = 2.2 \times 10^3$  and  $R \cdot k = 3.52 \times 10^5$  ( $k$  is the wave vector).

$$E \sim 2F \frac{J_1(x)}{x}; \quad x = 2\pi F \frac{r}{r_m}; \quad F = \frac{r_m^2}{\lambda L}. \quad (4)$$

Recall that  $r_m$  is the mirror radius. In the approximation of  $L \gg r_m$ , the polar angle  $\theta$  has been substituted for the radius  $r$  in the focal plane by the formula  $\theta \approx r/L$ . The example of calculations using formula (4) is presented in Fig. 3. The analytical expressions similar to (4) can be derived for some other initial distributions of the field. In the focus of the mirror, formulas (3) and (4) agree.

The resonator simulation based on expression (2) has some advantages. The calculations do not require substantial computational resources and a heavy time expense. This allows for the comparative research of the dynamics of the mode formation in the resonator to be carried out over a wide range of parameters. The method can be useful in investigating stable and unstable resonators with spherical, conical [15,16], and toroidal mirrors [17]. It can be applied for radiation either with homogeneous or radial (or azimuthal) polarization.

When calculating the integral (2), a correcting factor was introduced in each of the bounces. It was the same for the whole run of resonator calculations and was chosen by relying on the condition of the field amplitude reaching a constant value or a quasi-stationary state.

### 3. Calculation Results

Recall the known general regularities of the field behavior in a stable resonator observable in our calculations as well. After multiple reflections, a resonator with round mirrors exhibits the main LG TEM<sub>00</sub> mode. The specified initial distribution of the field does not affect the kind of attained stationary distribution of the field. The process of mode formation is characterized by the relaxation oscillations.

In consideration of the field evolution from the initial arbitrarily given distribution, attention should be paid to a number of factors:

- typical time of mode formation,
- amplitude of the field relaxation oscillations,
- period of the field relaxation oscillations,

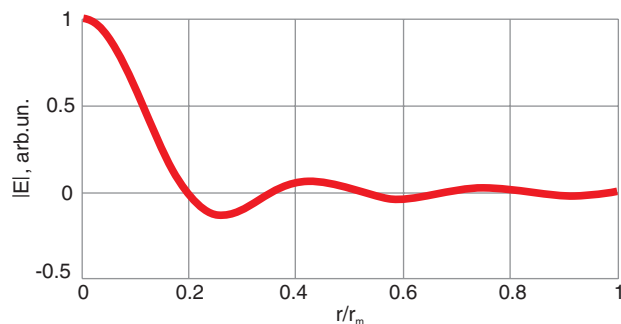


Fig. 3. (Color online) Amplitude of the field reflected from the mirror on the sphere of the  $L$  radius passing through the focus of the mirror as a function of the radius. Calculated parameters:  $r_m \cdot k = 2 \times 10^3$ ,  $L \cdot k = 2 \times 10^5$ , and  $R = 2 \cdot L$ .

- character of the field evolution to the mode, and
- type of the attained field distribution.

#### A. Oscillation Amplitude and Time of Mode Formation

A general idea of the speed of mode formation in the resonator is illustrated by Fig. 4. Three cases are presented here. The parameters  $g_i = 1 - \frac{L}{R_i}$ ;  $i = 1, 2$  are the same for all the variants, but the resonator length is different. The time of reaching a stationary distribution depends on Fresnel number  $F = \frac{r_m^2}{\lambda L}$ ,  $F = 2.39; 1.36; 0.96$  for the variants *a*, *b*, and *c*, correspondingly. In Fig. 4a the field oscillations are considerable, with a highly slow time evolution to the principal mode. Increasing  $L$ , we can observe a clear tendency toward mode formation, and in Fig. 4b, a stationary field is attained in several bounces.

However, a comparison of various resonator schemes proves that the above-cited Fresnel number is unsuitable for analyzing the time of mode formation (Fig. 5). In all three examples, the Fresnel number  $F = \frac{r_m^2}{\lambda L}$  is the same while the values of mode formation time are distinctly different. The time of attaining a field distribution in the resonator, corre-

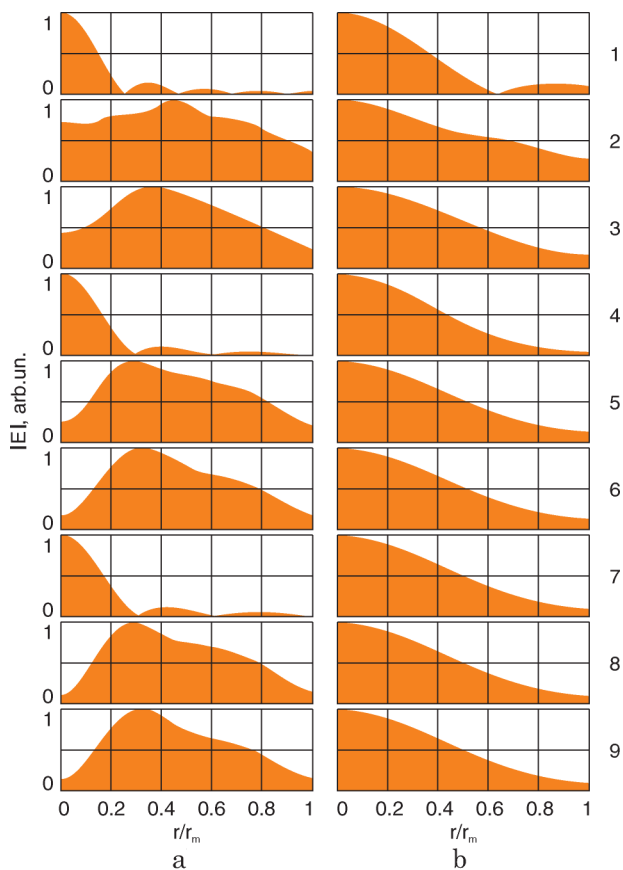


Fig. 4. (Color online) Radius dependence of the field amplitude at the mirror. The column of figures to the right shows the number of bounces. Dimensionless parameters:  $r_m \cdot k = 3 \times 10^3$  and  $R1 = R2 = 2 \cdot L$ . Two groups of curves correspond to different resonator lengths: a,  $L = 200 \cdot r_m$  and b,  $L = 500 \cdot r_m$ . The initial field amplitude is uniform; the front is flat.

sponding to the principal mode, is dependent on losses at the mirror edges, i.e., on the ratio between the caustic radius on the mirror and the radius of the mirror itself. The field has been calculated at  $r = 0.14 \cdot r_m$  (an arbitrarily chosen fixed radius). The  $x$  axis shows the number of full resonator bounces. Figure 5 in particular is indicative of the advantage of a convex–concave stable resonator: the time of mode formation here is minimal because this resonator displays the maximum caustic size of the main mode.

Figure 6 depicts the dependence of the field oscillation amplitude on the kind of initial distribution of the field. From the variants studied, the peak amplitudes of field fluctuations are observed in the initial field as plane waves (Fig. 6a). If we specify the front of the initial wave coinciding with the mirror surface and the distribution of the field amplitude corresponding to the TEM<sub>00</sub> mode for the given resonator configuration, the field fluctuations are absent. This quite reasonable conclusion concerns any resonator, including the configurations most unfavorable in terms of the time of mode formation. The specified distribution of the initial field is to be correlated with the structure of the active medium, and spontaneous emission from the active medium would be well taken as the initial one. We arrive at a quite clear recommendation that the structure of the active medium is best to be formed as being close in shape to the beam caustic. Actually, the beam quality of tube CO<sub>2</sub> lasers is better than that of fast-flow lasers with transverse pumping. In tube lasers, the bell-shaped distribution of the active medium is preferable in comparison with the uniform gain distribution from the point of view of the amplitude of field fluctuations.

#### B. Oscillation Period and the Character of Field Amplitude Evolution

In studying the period of field amplitude oscillations at the mirror, we were faced with the principal problem of the relationship between the wave and the geometric optics in the description of open resonators. It is a problem of the correlation of SP wave LG modes and MP geometric paraxial resonances.

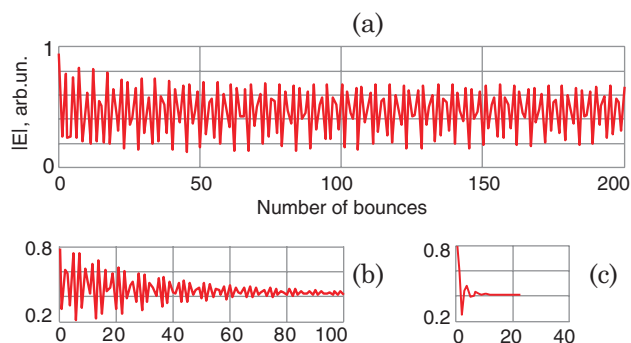


Fig. 5. (Color online) Field amplitude on the second mirror at  $r = 0.14 \cdot r_m$ . Parameters:  $r_m \cdot k = 2900$  and  $L = 195 \cdot r_m$ . The initial field amplitude is uniform; the front is flat. a,  $R1 = R2 = 2.5 \cdot L$ , b,  $R1 = 2.5 \cdot L$ ,  $R2 = \infty$ , and c  $R1 = 2.5 \cdot L$ ,  $R2 = -2.5 \cdot L$ .

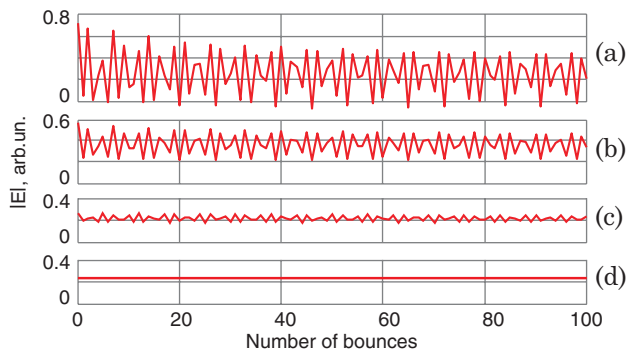


Fig. 6. (Color online) Evolution of the field amplitude on the second mirror at  $r = 0.14 \cdot r_m$ . Parameters:  $r_m \cdot k = 2900$ ,  $L = 2.12 \cdot r_m$ , and  $R1 = R2 = 2.6 \cdot L$ . The curves are for different initial field distributions. For a–c, the initial wavefront is flat. a, The field amplitude is uniform. b, The distribution is a Bessel function  $\sim J_0(2.405 \cdot r/r_m)$ . c, The distribution is a Gaussian function  $\sim \exp(-r^2/w_0^2)$ ,  $w_0/r_m = 0.413$ . d, The field distribution is the same as in the previous case. The wavefront coincides with the mirror surface.

The results of our calculations contain the qualitative effects of both approaches. We observe both paraxial resonances (at the corresponding configurations of resonators) and a SP lowest mode that is formed as a result of multiple reflections.

The period of field oscillations and the character of mode formation in the resonator differ sharply depending on the resonator parameters (Figs. 7 and 8). The field amplitude evolution can be aperiodic or manifest itself as beats of various frequencies. The parameters of resonators where beats are lacking in Fig. 7a conform with the condition of paraxial resonance derived in the context of resonator described by the methods of geometric optics [9]:

$$g_1 \cdot g_2 = \frac{1 + \cos \theta}{2}; \quad \theta = 2\pi \frac{K}{N}; \quad 0 \leq K \leq N/2, \quad (5)$$

where  $N$  is the number of resonator round trips required to form a closed ray trajectory.  $g_i = 1 - \frac{L}{R_i}$ ;  $i = 1, 2$  are the parameters of the stability diagram of the open resonators.

Beats take place at the resonator parameters slightly different from the conditions of paraxial resonance. The beat frequency (Figs. 7b and 7c) is related to the value of the mismatch.

The results of numerical calculations done in the context of the wave approach (Fig. 8) are uniquely indicative of the presence of paraxial resonance effects predicted in the geometric optics. The cases are illustrated when the oscillation period of the field corresponds to 3, 5, and 7 round trips of the resonator.

This phenomenon can be explained in the following way. The conclusions concerning paraxial resonances are applicable to the rays located at any distance from the axis; this is seen from formula (5) of paraxial resonance that involves no coordinates. However, there exist the boundaries of applicability of geometric consideration.

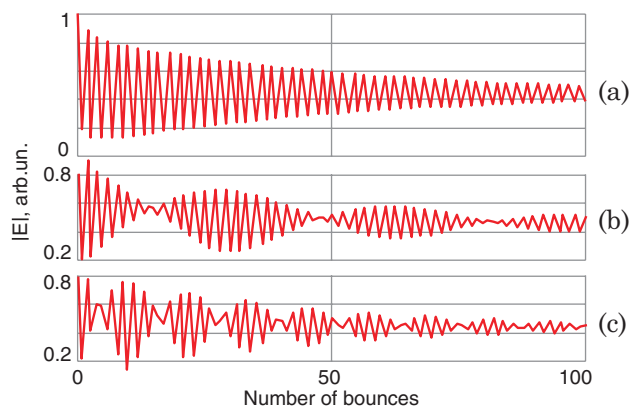


Fig. 7. (Color online) Evolution of the field amplitude on the second mirror at  $r = 0.14 \cdot r_m$ . Parameters:  $r_m \cdot k = 2900$  and  $L = 195 \cdot r_m$ . The second mirror is flat. The initial field amplitude is uniform; the front is flat. a,  $R1 = 2.0 \cdot L$ , b,  $R1 = 2.1 \cdot L$ , and c,  $R1 = 2.3 \cdot L$ .

A relatively large value of  $r(F = r^2/\lambda L > 1)$  permits paraxial resonances to be observed, but at small  $r(F \leq 1)$ , where the principal  $TEM_{00}$  mode is localized, the laws of geometric optics are inapplicable.

The important features of this effect should be noted. The resonances mentioned above can be observed independently on the mirror radius  $r_m$  and the initial field. These two factors can only influence the amplitude of oscillations or the time relaxation, but not the oscillation period.

The current results are expected to begin experimental research in this field. Two principal experiments that proved the existence of MP modes and paraxial resonances in the stationary state were performed in [9] by Ramsay and Degnan. In the first experiment, they measured the transparency of the passive resonator by changing its length. They obtained all the paraxial resonances predicted by the theory. The second experiment was performed on a  $CO_2$  laser with a variable resonator length. One manifestation of the paraxial resonances is apparent

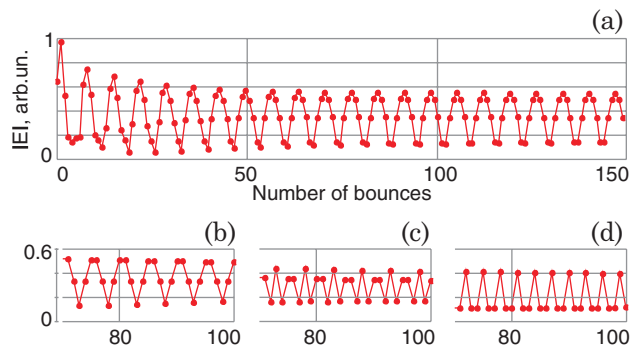


Fig. 8. (Color online) Examples of paraxial resonances. The field amplitude at the mirror center as a function of the number of bounces. The points on the curve correspond to consequent reflections from the mirror. a, Seven-pass resonance at  $g_1 = g_2 = 0.222$ . b, Five-pass resonance at  $g_1 = g_2 = 0.309$ . c, Five-pass resonance at  $g_1 = g_2 = 0.809$ . d, Three-pass resonance at  $g_1 = g_2 = 0.5$ .

in the power profiles of hole-coupled lasers. Measured output power against mirror separation for a hole-coupled CO<sub>2</sub> laser shows dips in the power. These dips occur at the paraxial resonance positions given by the corresponding formulas.

### C. Laguerre–Gaussian Nonzero Modes

The problem of high-order LG modes is of considerable interest. The accepted classification of lasers in the world market (both low power, e.g., He–Ne lasers, and high power, such as CO<sub>2</sub> lasers) with regard to mode composition is strange, as only two variants are usually offered: single-mode (the main TEM<sub>00</sub> mode) lasers or multimode lasers. The situation is clarified by Fig. 9, which depicts the results of the calculation for a specified resonator configuration using the initial radiation that ideally corresponds to the TEM<sub>10</sub> mode both in the front shape and the field distribution. In this ideal case, the TEM<sub>10</sub> mode persists, and no relaxation oscillations are observed.

Nevertheless, any deviations of the initial field from the ideal one cause a cardinal change in the situation. In Fig. 9b, the front of the initial field is only varied as against Fig. 9a; now it is flat. The initial distribution appropriate for the TEM<sub>10</sub> mode is “decomposed” and evolves to the principal TEM<sub>00</sub> mode via relaxation oscillations. The character of field evolution shown in Fig. 9b is qualitatively retained at other differences from the ideal case (Fig. 9a), such as with the variations in  $w_0$ . For Fig. 9a, the value of  $w_0$  is derived from the known formulas as a function of the resonator parameters. Mention is made that the time of mode formation depends on diffraction losses at the mirror edges and, hence, on the mirror radius. On reducing the mirror radius, the above-cited qualitative behavior of the field is retained.

The reason for this behavior of the field is that with the Fresnel number  $F = r^2/\lambda L$  exceeding unity, the SP higher order LG modes cannot compete with the MP modes of the paraxial resonances resulting from geometric optics. The MP modes are known not to show a certain distribution of field in the cross section, so their formation does not take much time when compared with LG modes. On the other hand, the similar typical size of the field along the mirror

radius SP LG modes exhibits higher diffraction losses at the mirror edges than the MP modes of geometric optics. The first ones have the same, comparatively high losses at the mirror edges on each pass. The radius of the MP modes is changed cyclically; therefore, the MP averaged losses of these modes are lower. The exception is the principal TEM<sub>00</sub> mode, in the scope of which a consideration in terms of the beam is not applicable.

The results of calculation suggest that it is not correct to consider output radiation of a nonprincipal mode laser to be “multimode.” Actually, any distribution of the field amplitude in the waist (if the phase is constant) can be formally expanded into a series of real orthogonal LG functions. It does not mean, however, that any laser beam can be presented as a superposition of LG TEM<sub>pq</sub> modes. The complex functions describing LG modes are not orthogonal at the nonzero phase shift between two functions. We also cannot guarantee that the beam of the real “multimode laser” has a waist with the constant phase over the beam cross section.

In the most practical cases, the real beam is not finally formed either as the single-mode LG beam or as the coherent superposition of low-order LG modes. One possible reason is low resonator quality; another reason is not enough time for mode formation in pulsed lasers. In both cases, we cannot hope that the phase is constant in the waist so we cannot even follow the procedure described above.

Actually, the laser beam in a “multimode laser” contains a considerable portion of “MP geometric modes” with an uncertain structure of the field in the cross section. The portion of this component is governed by the Fresnel number. The deviation from the paraxial resonance does not bring about a critical change in the situation; generation of a proper LG mode of the order above zero (or a superposition of low-order modes) is not possible. The mode of oscillation suggests that a deviation from the resonance is responsible for simultaneous excitation of two or more closely spaced resonances of lower quality.

At the same time, it would be desirable in many cases to realize the generation of a specific nonzero LG mode displaying the predicted features, instead

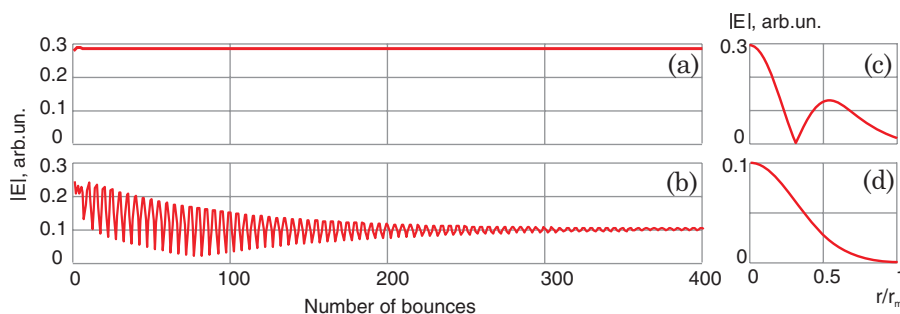


Fig. 9. (Color online) Effect of the kind of the initial field distribution upon the mode formation. Temporal evolution of the field at the center of the mirror a, b, radial distribution of the field in the c, d, steady state mode. Parameters:  $r_m \cdot k = 2450$ ,  $L = 231 \cdot r_m$ , and  $g_1 = g_2 = 0.309$ . a, The initial wave has a wavefront matching the mirror surface and the field distribution in the form of the TEM<sub>10</sub> mode at  $w_0 = 0.445 \cdot r_m$ . b, The same parameters as in a, except for the wavefront; here it is flat.

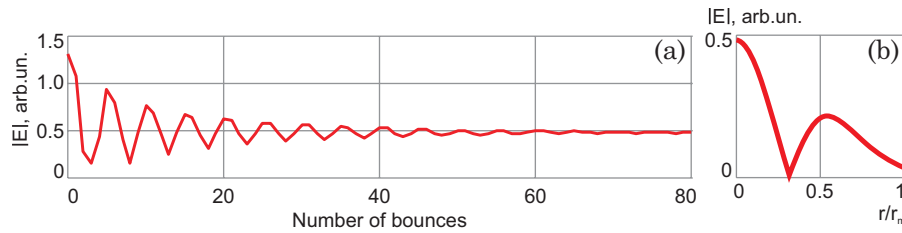


Fig. 10. (Color online) Effect of the absorbing mask at the mirror upon mode formation. a, Temporal evolution of the field at the center of the mirror and b, radial distribution of the field in the steady state mode. Parameters:  $r_m \cdot k = 2450$ ,  $L = 231 \cdot r_m$ , and  $g_1 = g_2 = 0.309$ . The initial field amplitude is uniform; the front is flat. The radius of the absorbing ring is  $w_1/\sqrt{2} = 0.31 \cdot r_m$ ; it coincides with the zero field location for the  $TEM_{10}$  mode. The area of the absorbing ring comprises 1% of that of the mirror.

of “multimode” generation. This can be effectively achieved (for at least the low-order modes) by applying a mask to the resonator mirror. Entering an absorbing annular zone on the mirrors in our numerical experiments resulted in a suppression of MP modes and in the generation of a  $TEM_{10}$  mode (Fig. 10). The radius of the absorbing ring equaled that of the zero field of the  $TEM_{10}$  mode, and the area of the ring comprised less than 1% of the mirror area. In the absence of the absorbing ring, relaxation oscillations gave rise to formation of the principal  $TEM_{00}$  mode, the time of achieving the stationary filled distribution being considerably longer.

#### 4. Conclusion

One-dimensional resonator simulation for the axially symmetric field distribution has been developed. It is intended to be used in studying the dynamics of field distribution formation in empty resonators. The model employs an analytical description of radiation diffraction from a narrow ring slit. Reflection of an incident wave with a specified amplitude-phase distribution from the mirror is calculated by the Green function method.

The process of mode formation is shown to have the different character of relaxation oscillations, depending on the resonator parameters. The evolution of the relaxation oscillation amplitude can be aperiodic or occur as beating. The wave-based resonator simulation reveals “paraxial resonances” predicted in [9] by the methods of ray optics. It has been shown that the conditions of paraxial resonance are matched by aperiodic processes of evolution of relaxation oscillation amplitude in the course of mode formation. Deviations of the resonator parameters from the conditions of paraxial resonance cause a qualitative change in the character of oscillations. The monotonically damping amplitude of the field oscillations gives place to damped beats. Their period is dependent on the value of the resonator parameter deviation from the conditions of “paraxial resonance.” Some parameters of the resonator are accompanied by more complex oscillations close to chaotic ones. In this case, oscillations involve two or several “paraxial resonance modes,” their quality being comparable for the given resonator configuration.

The time of mode formation is defined by the quantity of diffraction losses at the mirror edges. The re-

laxation oscillation amplitude is governed by the field initial distribution.

An efficient means of  $TEM_{10}$  mode generation, the principal mode and MP geometric mode suppression, is employing a mask on the resonator mirror. It is made as a ring of zero reflection and placed in the area of the  $TEM_{10}$  mode zero field. In such a resonator, the  $TEM_{10}$  mode is formed much faster than the stationary generation is reached in the absence of an absorbing mask on the mirror.

We would call attention once again to the advantages of employing convex–concave stable resonators showing the best parameters for the resonator filling with the caustic of the principal mode [3,18]. To this, one can add a fast evolution of the initial field to the mode (Fig. 5c). The problem of parallel beam extraction from the resonator containing spherical mirrors is solved by fitting a curvature of the outer antireflective surface of the output mirror. With regard to its “increased sensitivity” to misalignment, this problem is exaggerated. It is evident from the simplest comparative estimations by the formulas of [3] for the resonators with the similar volumes of the mode.

The results of this paper should be taken into account in operating low-quality stable resonators in high-power cw lasers and in pulsed lasers.

#### Appendix A: Wave Reflection from the Round Mirror of Finite Dimensions

Deriving an integral for calculation of a reflected wave resulting from radiation incidence on the round mirror of finite dimensions presented here is performed for an axially symmetric case and in paraxial approximation.

Assume that a distribution of the initial field of linear polarization  $E'(\rho', \varphi', z')$  is specified on the flat surface of a round mirror  $S'(\rho', \varphi')$ . Radiation is directed onto the mirror along its axis. The scalar Kirchhoff integral for the electric field can be written in its general form as

$$E(\mathbf{r}) = \int_0^{2\pi} \int_0^r (G(|\mathbf{r} - \mathbf{r}'|) \frac{\partial}{\partial z'} E'(\rho', \varphi', z') - E'(\rho', \varphi', z') \frac{\partial}{\partial z'} G(|\mathbf{r} - \mathbf{r}'|)) \rho' \cdot d\varphi' \cdot dr',$$

where  $\mathbf{r}(r, \varphi, \theta)$  is the radius vector directed from the origin of coordinates (at the mirror center) to the point of diffraction field calculation,  $\rho'$  and  $\varphi'$  are the polar coordinates on the mirror surface,  $\mathbf{r}'(\rho', \varphi')$  is the radius vector on the mirror surface directed from the origin of coordinates to the emitting point, and  $G = \frac{e^{ik|r-\mathbf{r}'|}}{|r-\mathbf{r}'|}$  is the field of the point source.

Consider now the axially symmetric problem. The initial field is given as  $E'(\rho', \varphi', z') = E_0(\rho') \cdot e^{ikz'}$ . Then  $\frac{\partial}{\partial z'} E'(\rho', z')|_{z'=0} = ikE_0(\rho')$ . For the wave zone ( $kr \gg 1$ )  $\frac{\partial}{\partial z'} G \approx ikG \frac{\partial}{\partial z'} |r-\mathbf{r}'|$ , and the integral will take the form

$$E = ik \int_0^{2\pi} \int_0^{r_m} GE_0(\rho') \cdot \left(1 - \frac{\partial}{\partial z'} |r-\mathbf{r}'|\right) \rho' \cdot d\varphi' \cdot d\rho'.$$

The conclusion is made for the resonators with the mirror radii  $r_m$  much smaller than the distance between them. Thus, both the dimensions of the emitting zone and the size of the diffraction pattern calculation region are much less than the distance at which the diffraction pattern is calculated. In view of this, we can write

$$\begin{aligned} |\mathbf{r}-\mathbf{r}'| &\approx r \left(1 - \frac{x \cdot x' + y \cdot y'}{r^2} + \frac{x'^2 + y'^2}{2 \cdot r^2}\right) \\ &= r \left(1 - \frac{\rho'}{r} \sin \theta \cos(\varphi - \varphi') + \frac{\rho'^2}{2 \cdot r^2}\right). \end{aligned}$$

Here ( $x, y, x', y' \ll r$ ),  $\frac{\rho'}{r} \ll 1$ ,  $\sin \theta \ll 1$ . So in further transformations of integration elements,  $|\mathbf{r}-\mathbf{r}'|$  can be substituted for  $r$  everywhere except for the exponent in  $G$  that describes the phase. Substituting  $\frac{\partial}{\partial z'} |r-\mathbf{r}'|_{z'=0} \approx -\frac{z}{r} = -\cos \theta \approx -1$ , we can write further:

$$\begin{aligned} E(\mathbf{r}) &= 2ik \int_0^{r_m} \int_0^{2\pi} GE_0(\rho') \cdot \rho' \cdot d\varphi' \cdot d\rho' \\ &= 2ik \int_0^{r_m} E_0(\rho') \int_0^{2\pi} \frac{e^{ik|r-\mathbf{r}'|}}{|r-\mathbf{r}'|} \rho' \cdot d\varphi' \cdot d\rho' \\ &\approx 2ik \frac{e^{ikr}}{r} \int_0^{r_m} E_0(\rho') \int_0^{2\pi} e^{-ik\rho' \sin \theta \cos(\varphi-\varphi')} e^{ik\frac{\rho'^2}{2r}} \rho' \cdot d\varphi' \\ &\quad \cdot d\rho' \\ &= 2ik \frac{e^{ikr}}{r} \int_0^{r_m} E_0(\rho') e^{ik\frac{\rho'^2}{2r}} J_0(k\rho' \sin \theta) \rho' d\rho'. \end{aligned}$$

Here, a known formula  $J_0(x) = \frac{1}{\pi} \cdot \int_0^\pi e^{-ix \cos t} dt$  is used,  $r_m$  is the mirror radius.

The derived expression can be interpreted in terms of the Green function approach, where the formula for diffraction from a narrow ring slit of  $r_0$  radius has the form

$$\text{DEL}(L, \theta, r_0) \approx 2\pi r_0 ik \frac{e^{ikL}}{L} e^{ik\frac{r_0^2}{2L}} J_0(kr_0\theta).$$

Here the denotation  $r$  for the distance between the aperture and the observation point is changed for  $L$  (the distance between the resonator mirrors). For any axially symmetric amplitude-phase distribution of the incident field  $E_0(r_0)$ , the diffraction field is calculated using the integral

$$E(L, \theta) \sim \int_0^{r_m} r_0 E_0(r_0) \text{DEL}(L, \theta, r_0) \exp\left(-ik \frac{r_0^2}{R}\right) dr_0.$$

A multiplier having the form of an exponent describes an additional phase shift related to the mirror curvature  $R$ . This phase shift emerges as incident radiation  $E_0(r_0)$  reflected from the mirror.

The formula of diffraction from a narrow ring at azimuthal (radial) polarization is obtained in a similar way [19]:

$$\text{DEA}(L, \theta, r_0) \approx 2\pi r_0 ik \frac{e^{ikL}}{L} e^{ik\frac{r_0^2}{2L}} J_1(kr_0\theta).$$

Calculation of the diffraction field of the whole mirror will require the same integral with a substitution of  $\text{DEL}(L, \theta, r_0)$  for  $\text{DEA}(L, \theta, r_0)$ .

The authors express their thanks to M. D. Khomenko for his contribution in performing calculations.

## References

1. A. G. Fox and T. Li, "Resonant modes in a maser interferometer," *Bell Syst. Tech. J.* **40**, 453–458 (1961).
2. H. Kogelnik and T. Li, "Laser beams and resonators," *Appl. Opt.* **5**, 1550–1567 (1966).
3. A. E. Siegman, *Lasers* (University Science, 1986).
4. N. Hodgson and H. Weber, *Optical Resonators: Fundamentals, Advanced Concepts and Applications* (Springer Verlag, 1997).
5. Y. A. Anan'ev, *Laser Resonators and the Beam Divergence Problem* (Institute of Physics Publishing, 1992).
6. H. A. Haus *Waves and Fields in Optoelectronics* (Prentice-Hall, 1984).
7. S. Solimeno, B. Crosignani, and P. Guiding DiPorto, *Diffraction and Confinement of Optical Radiation* (Academic, 1986).
8. A. A. Ishaaya, N. Davidson, and A. A. Friesem, "Very high-order pure Laguerre–Gaussian mode selection in a passive Q-switched Nd:YAG laser," *Opt. Express* **13**, 4952–4962 (2005).
9. I. A. Ramsay and J. J. Degnan, "A ray analysis of optical resonators formed by two spherical mirrors," *Appl. Opt.* **9**, 385–398 (1970).

10. C. H. Chen, P. T. Tai, M. D. Wei, and W. F. Hsieh, "Multibeam-waist modes in an end-pumped Nd:YVO<sub>4</sub> laser," *J. Opt. Soc. Am. B* **20**, 1220–1226 (2003).
11. H. H. Wu and W. F. Hsieh, "Observations of multipass transverse modes in an axially pumped solid-state laser with different fractionally degenerate resonator configurations," *J. Opt. Soc. Am. B* **18**, 7–12 (2001).
12. C. H. Chen and C. F. Chiu, "Generating a geometric mode for clarifying differences between an operator method and SU(2) wave representation," *Opt. Express* **15**, 12692–12698 (2007).
13. C. H. Chen, P. Y. Huang, and C. W. Kuo, "Geometric modes outside the multi-bouncing fundamental Gaussian beam model," *J. Opt.* **12**, 015708 (2010).
14. J. Dingjan, M. P. Exter, and J. P. Woerdman, "Geometric modes in a single-frequency Nd:YVO<sub>4</sub> laser," *Opt. Commun.* **188**, 345–351 (2001).
15. N. K. Anatol, G. E. Katranji, and A. R. Anatol, "Axicon-based Bessel resonator: analytical description and experiment," *J. Opt. Soc. Am. A* **18**, 1986–1992 (2001).
16. E. F. Yelden, H. J. J. Seguin, C. E. Capjack, S. K. Nikumb, and H. Reshef, "Toric unstable CO<sub>2</sub> laser resonator: an experimental study," *Appl. Opt.* **31**, 1965–1974 (1992).
17. M. Endo, "Azimuthally polarized 1 kW CO<sub>2</sub> laser with a triple-axicon retroreflector optical resonator," *Opt. Lett.* **33**, 1771–1773 (2008).
18. X. Li, Y. Chen, T. Li, Y. He, Y. Gao, H. Cao, and S. Deng, "Development of red internal mirror He–Ne lasers with near-critical concave–convex stable resonator," *Proc. SPIE* **2889**, 358–366 (1996).
19. A. V. Nesterov and V. G. Niziev, "Vector solution of the diffraction task using the Hertz vector," *Phys. Rev. E* **71**, 046608 (2005).